Induced Drag Calculations with the Unsteady Vortex Lattice Method for Cambered Wings

Thomas Lambert*, Grigorios Dimitriadis†,

Aerospace and Mechanical Engineering Department,

University of Liège, 4000 Liège, Belgium

Nomenclature

A	=	panel area, m^2
b	=	semichord, m
c	=	chord, m
C_d	=	sectional drag coefficient
C_l	=	sectional lift coefficient
D	=	panel drag, N
$\mathbf{F}$	=	force vector, N
h	=	plunge displacement, m
k	=	reduced frequency
L	=	panel lift, N
$\mathbf{l}$	=	vortex segment vector
M	=	number of chordwise panels
N	=	number of spanwise panels
$\mathbf{n}$	=	panel normal vector
P	=	orthogonal projection operator
s	=	nondimensional time
$\mathbf{U}$	=	velocity vector, $m \cdot s^{-1}$
t	=	time, s
α	=	angle of attack, rad
Δb	=	panel span, m
Δc	=	panel chord, m
Δp	=	pressure drop
Γ	=	circulation, $m^2 \cdot s$
ω	=	angular velocity, $rad \cdot s^{-1}$

*PhD Student, Aerospace and Mechanical Engineering Department, t.lambert@ulg.ac.be

†Associate Professor, Aerospace and Mechanical Engineering Department, AIAA Senior Member, gdimitiradis@ulg.ac.be

ρ_∞	=	freestream air density, $\mathrm{kg \cdot m^{-3}}$
$\boldsymbol{\tau}$	=	panel tangential vector

Subscript

i	=	panel index in the chordwise direction
j	=	panel index in the spanwise direction

Superscripts

$(\dot{\ })$	=	time derivative
$(\hat{\ })$	=	unit vector
$(\bar{\ })$	=	amplitude

I. Introduction

The Unsteady Vortex Lattice Method (UVLM) [1] is an approach widely used to estimate the aerodynamic loads in unsteady subsonic flows. It is based on modeling the camber surface of a lifting body by means of bound vortex rings. Additional vortex rings are shed at the trailing edge in order to model the wake. Even though this method has been known and used for several decades, there is little discussion of the modeling of the leading-edge suction in the literature. To address this concern, Simpson *et al.* [2] presented a comparison of two different ways to model this effect for the case of uncambered airfoils and wings in harmonic pitch or plunge motions of small amplitude. One method was found to converge significantly faster than the other.

The present note is an extension of the study by Simpson *et al.* to cambered lifting surfaces. It shows that the presence of camber changes radically the convergence performance of the two methods.

II. Method

Simpson *et al.* studied two approaches for calculating the aerodynamic forces for the UVLM. The first one, based on the theory of circulatory forces is referred to as the *Joukowski* method in their paper; the second one, developed by Katz and Plotkin [1] is based on the computation of the pressure jump across the airfoil and is referred to as the *Katz* method. For convenience, the same terminology will be employed here.

A. Joukowski method

This procedure requires the calculation of the force contributions of all the bound vortices in order to model the effects of leading-edge suction. The total force generated by each vortex ring is divided in two parts: (quasi)steady and unsteady. The steady contribution of one vortex segment

m is simply calculated from the Joukowski theorem as:

$$\mathbf{F}_m^{\text{st}} = \rho_\infty \Gamma_m (\mathbf{U}_m \times \mathbf{l}_m) \tag{1}$$

with $\mathbf{l}_m$ the vortex segment vector, $\mathbf{U}_m$ the local flow velocity evaluated at the center of the segment and Γ_m the circulation of that segment. In general, the circulation of each segment is equal to the circulation of the panel: $\Gamma_m = \Gamma_{ij}$; the only exception is for the segments of the trailing edge, where the circulation of the first wake segments (Γ_{1j}^w) must be subtracted: $\Gamma_m = \Gamma_{ij} - \Gamma_{1j}^w = 0$ (*Kutta* condition).

The unsteady contribution arises from the unsteady part of Bernoulli's equation and acts along the normal $\mathbf{n}$ of each vortex ring panel [5]

$$\mathbf{F}_{ij}^{\text{unst}} = \rho_\infty \frac{\partial \Gamma_{ij}}{\partial t} A_{ij} \mathbf{n}_{ij} \tag{2}$$

with A_{ij} the panel's area. Finally the total force contribution from the whole panel can be calculated from the steady contribution of each of its vortex segments and the unsteady contribution of the panel:

$$\mathbf{F}_{ij}^{\text{tot}} = \sum_{m=1}^{4} \mathbf{F}_m^{\text{st}} + \mathbf{F}_{ij}^{\text{unst}} \tag{3}$$

B. Katz method

For this method, the unsteady Bernoulli equation is used to determine the pressure jump across each panel:

$$\Delta p_{ij} = \rho_\infty \left((\mathbf{U}_{ij}^m + \mathbf{U}_{ij}^w).\boldsymbol{\tau}_{ij}^c \frac{\Gamma_{ij} - \Gamma_{i-1,j}}{\Delta c_{ij}} + (\mathbf{U}_{ij}^m + \mathbf{U}_{ij}^w).\boldsymbol{\tau}_{ij}^s \frac{\Gamma_{ij} - \Gamma_{i,j-1}}{\Delta b_{ij}} + \frac{\partial \Gamma_{ij}}{\partial t} \right) \tag{4}$$

where $\mathbf{U}_{ij}^m$ is the velocity due to the surface motion and $\mathbf{U}_{ij}^w$ is the velocity due to the wake vorticity, all taken at the panel's collocation point. The bound vorticity contribution is approximated by the gradient of circulation along the direction of the panel's tangential vectors, $\boldsymbol{\tau}_{ij}^c$ and $\boldsymbol{\tau}_{ij}^s$ respectively for the chordwise (Δc_{ij}) and spanwise (Δb_{ij}) directions. The lift can be computed from

$$\Delta L_{ij} = \Delta p_{ij} A_{ij} \cos(\alpha_{ij}) \tag{5}$$

with α_{ij} the panel's angle of attack.

This procedure is only valid for the lift calculation since it does not account for the leading-edge suction force, overestimating the drag [1]. Instead of using the pressure difference for the calculation of induced drag, Katz and Plotkin define the drag as the force component parallel to the flight direction. After calculating the component of downwash that acts along the local lift vector, each panel's contribution to the induced drag is given by

$$\Delta D_{ij} = \rho_\infty \left((\mathbf{U}_{ij}^{bc} + \mathbf{U}_{ij}^{w}).(P_{\widehat{\mathbf{U}}_{ij}^m}\mathbf{n}_{ij})(\Gamma_{ij} - \Gamma_{i-1,j})\Delta b_{ij} + \frac{\partial \Gamma_{ij}}{\partial t} A_{ij} \sin(\alpha_{ij}) \right) \tag{6}$$

with $\mathbf{U}_{ij}^{bc}$ the velocity at the panel's collocation point calculated considering only the bound chordwise vortices. The second term arises from the unsteady Bernoulli equation. The term $(P_{\widehat{\mathbf{U}}_{ij}^m}\mathbf{n}_{ij})$ is an orthogonal projection of the normal to the panel in the plane of the flow and therefore it ensures that only the downwash component of the velocities is taken [2]. The projection operator is defined as $P_{\widehat{\mathbf{U}}_{ij}^m} = I - \widehat{\mathbf{U}}_{ij}^m \widehat{\mathbf{U}}_{ij}^{m^T}$, where the unit vector $\widehat{\mathbf{U}} = \mathbf{U}/|\mathbf{U}|$ describes the direction of the local flow velocity. Finally, the total aerodynamic load acting on each panel is

$$\mathbf{F}_{ij}^{\mathrm{tot}} = \Delta D_{ij} \widehat{\mathbf{U}}_{ij}^m + \Delta L_{ij}(P_{\widehat{\mathbf{U}}_{ij}^m}\mathbf{n}_{ij}) \tag{7}$$

C. Comments

The two methods have each their drawbacks and advantages. Moreover, only the chordwise-oriented segments contribute to $\mathbf{U}_{ij}^{bc}$ with the Katz method, which can also lead to approximation errors, especially in the presence of cross wind. On the other hand, the Katz approach is less computationally expensive than the Joukowski method. For a given discretisation of M chordwise and N spanwise panels, the number of points required for the calculation of velocities with the Katz method is

$$n_{\mathrm{points}} = M \times N \tag{8}$$

while for the Joukowski method the number of points is

$$n_{\mathrm{points}} = \underbrace{(M+1) \times N}_{\text{spanwise segments}} + \underbrace{(N+1) \times M}_{\text{chordwise segments}} \tag{9}$$

In general, the Joukowski method will require approximately three times more computing effort because it calculates the local velocities at more than twice the points than the Katz technique.

III. Results

The two methods were first applied to a 2D uncambered airfoil and benchmarked against the analytical solution by Theodorsen [4] and Garrick [3], as was done by Simpson *et al.*. Excellent agreement with the analytical solutions was obtained. Then, the convergence of the two methods was analyzed for airfoils and finite wings of different camber.

A. Kinematics

Two motions are studied: harmonic plunging, specified by $h = \overline{h}\cos(ks)$ and harmonic pitching, described by $\alpha = \overline{\alpha}\sin(ks)$; where $\overline{h}$ and $\overline{\alpha}$ are oscillating amplitudes, $s = U_\infty t/b$ is a nondimensional time and $k = \omega b/U_\infty$ is the reduced frequency. The downwash induced by the motions depends on $\dot{h}$, α and $\dot{\alpha}$, all of which can be calculated analytically.

All the cases studied in this note involve a prescribed wake, i.e. the wake panels are convected with the free stream velocity. To ensure that the newly shed wake panels have the same area as the bound panels, the time step is set to $\Delta t = c/(U_\infty M)$ [2]. In order to avoid disturbances due to the impulsive start of the flow, the simulation is conducted until the wake length reaches 25 times the chord length or until at least two complete cycles of oscillation are simulated, whichever is longer. The results presented hereafter correspond to the values over the last cycle.

B. 2D Airfoils

For 2D flow cases the wing is modelled with an extremely large aspect ratio ($AR = 4000$) and without any spanwise discretisation ($N = 1$); this ensures that the wing tip effects remain negligible, and thus the problem is quasi 2D [2].

Simpson *et al.* [2] already showed that both methods present a good match to the linear theory. A convergence study can be carried out for the two methods. Here, this analysis is performed with respect to the chordwise discretisation only. The error in the drag coefficient estimate C_d is computed as

$$\text{error}(M) = \frac{\text{RMS}\left[C_d(M_{\max}) - C_d(M)\right]}{\max\limits_t |C_d(M_{\max})|} \times 100 \qquad [\%] \tag{10}$$

The finest discretisation is set to 50 chordwise panels ($M_{\max} = 50$), as this value results in adequately converged aerodynamic load predictions. The convergence of the two methods is compared on two airfoils, one uncambered and one with the NACA 64xx camber line. The results are presented in Fig. 1a and 1b , which plots the variation of error in C_d prediction against M for the uncambered airfoil and two values of the reduced frequency. Convergence is very fast in the plunge case but the Joukowski method performs better than the Katz approach. In pitch however there is very little difference in the convergence of the two methods (the Joukowski method is marginally faster for the first few values of M tested, but rapidly the difference in error becomes negligible).

For the cambered plate (Fig. 1c and 1d) the results are quite different. For both reduced frequencies, the Joukowski method presents a small advantage over the Katz technique, but only in plunge. In pitch, the Katz approach is marginally faster. Similar behaviours were observed at reduced frequency values of $k = 0.2$ and $k = 0.8$. Other cambered profiles were studied (NACA 14xx, 24xx, 34xx, 44xx, 54xx) for a reduced frequency of $k = 0.2$. For all these profiles, the Katz approach converges faster in pitch, but the Joukowski method is slightly faster in plunge.

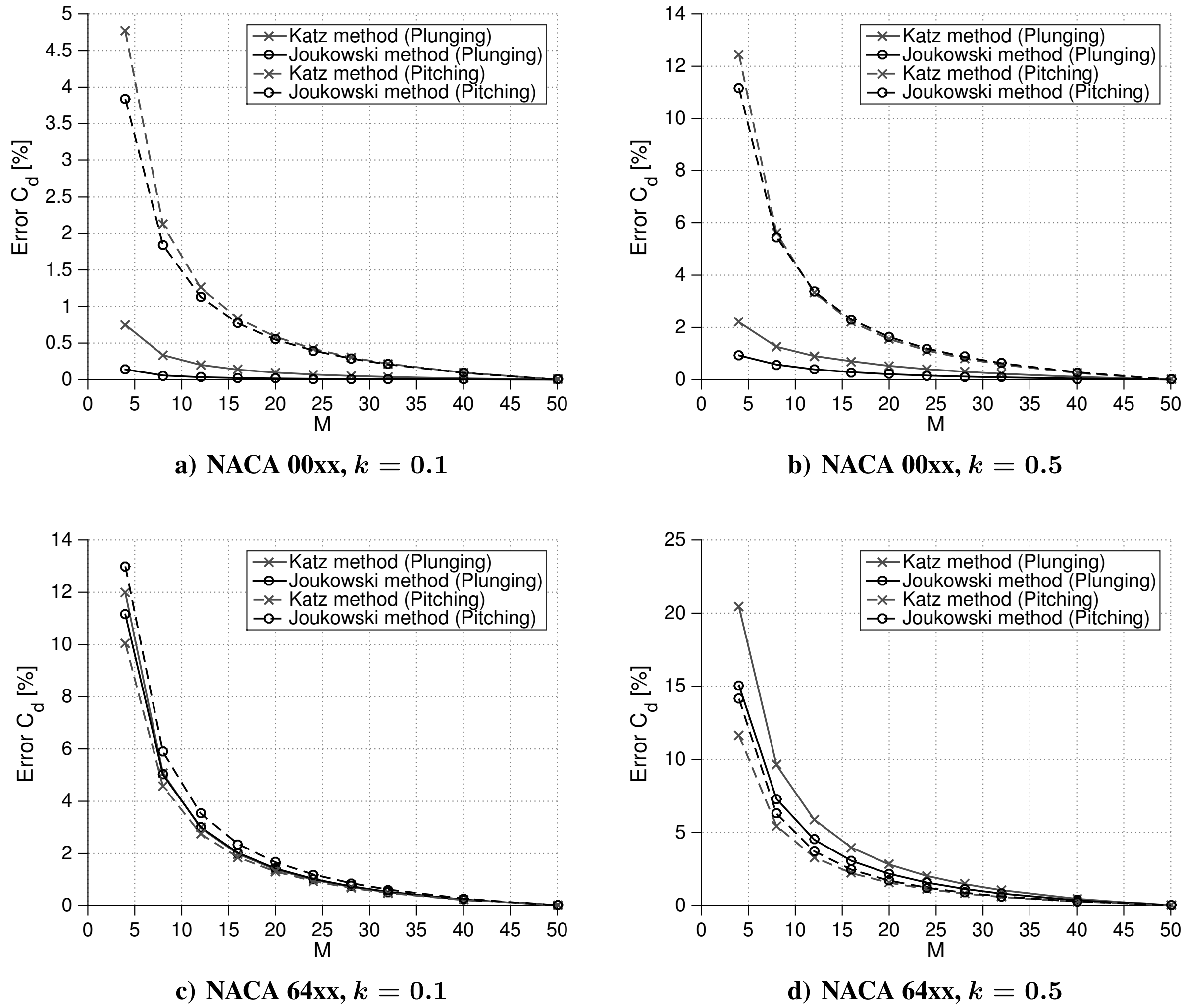

a) NACA 00xx, $k = 0.1$

b) NACA 00xx, $k = 0.5$

c) NACA 64xx, $k = 0.1$

d) NACA 64xx, $k = 0.5$

Figure 1. Convergence for pitching and plunging at $k = 0.1$ and at $k = 0.5$, for uncambered and cambered airfoils.

Moreover, the difference in convergence rate was found to decrease with camber in pitch, while no significant difference was found for the plunging motion. In general, convergence is slower for high camber values due to a poorer approximation of the cambered surface by linear panels. The approximation becomes particularly poor when $M < 10$, as the collocation points lie significantly below the camber line.

C. 3D wings

The same pitch and plunge kinematics are used for finite wings as for 2D airfoils. The aspect ratio is set to $AR = 4$ and the number of spanwise panels is set to $N = 24$. Convergence tests are carried out on two finite wings, one uncambered and one with the NACA 64xx camber line. The error in drag coefficient is again calculated using equation 10 and is plotted against M in Fig. 2 for pitching or plunging wings at two reduced frequencies. For the uncambered wing (Fig. 2a and 2b),

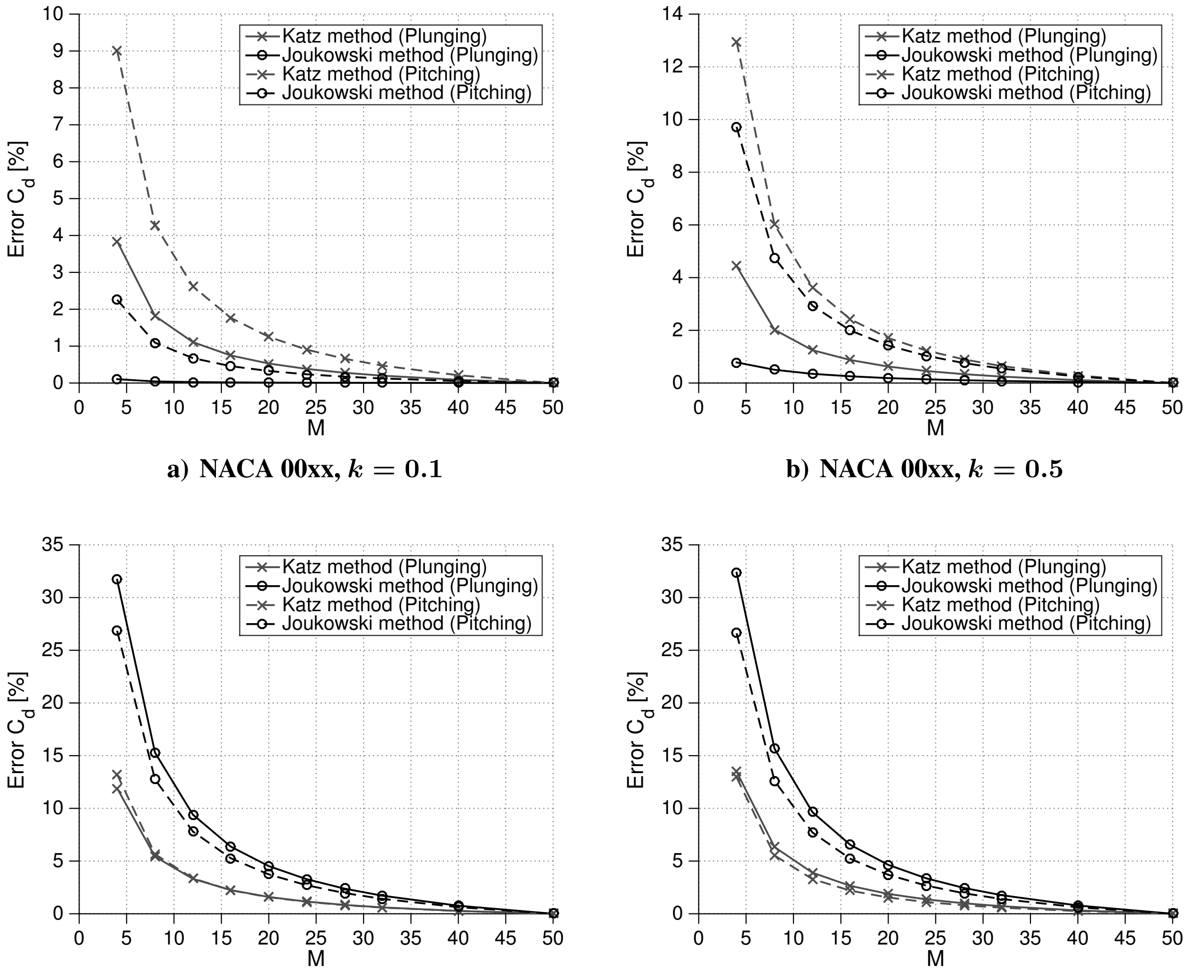

a) NACA 00xx, $k = 0.1$ b) NACA 00xx, $k = 0.5$

c) NACA 64xx, $k = 0.1$ d) NACA 64xx, $k = 0.5$

Figure 2. Convergence for pitching and plunging at $k = 0.1$ and at $k = 0.5$, for uncambered and cambered finite wings.

the conclusions drawn by Simpson *et al.* [2] are confirmed. The Joukowski method converges even faster than in the 2D case, although the convergence rate decreases with increasing reduced frequency (this slowdown was confirmed by carrying out additional simulations at $k = 0.2$ and $k = 1$). At high values of the reduced frequency, the added mass component of the aerodynamic loads becomes dominant. As added mass effects are uniform over the span, the convergence pattern becomes similar to the one observed in the 2D case for high k.

The results are markedly different for the cambered wing (Fig. 2c and 2d). The convergence of the Katz approach is found to be notably faster than that of the Joukowski method, both in pitch and in plunge. Furthermore, as in the 2D case, the reduced frequency and kinematics seem to have little influence on the convergence rate of the two approaches. Other cambered wings (NACA 00xx, 14xx, 24xx, 34xx, 44xx, 54xx, 64xx) of aspect ratio $AR = 4$ and reduced frequency $k = 0.2$ were also investigated. In all cases it was found that the Katz method was converging significantly faster in both pitch and plunge. The variation of the error on the drag coefficient with camber is shown in Fig. 3. The results presented in this figure are for finite wings of $AR = 4$, pitching or plunging at a reduced frequency of $k = 0.2$ and for a chordwise discretisation of $M = 28$. It is clear that in both cases, the error of the Katz method is higher for uncambered wings but becomes lower than the Joukowski error as soon as camber is introduced. In general, the difference in error is increasing with camber, leading to a clear advantage for the Katz method. The lack of monotonicity may arise from the fact that the errors presented here are relative to a

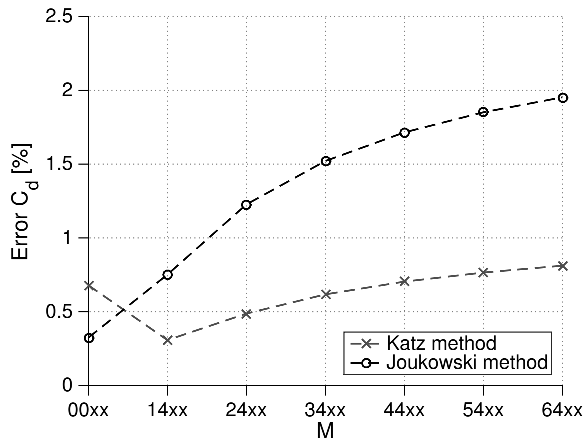

a) Pitch

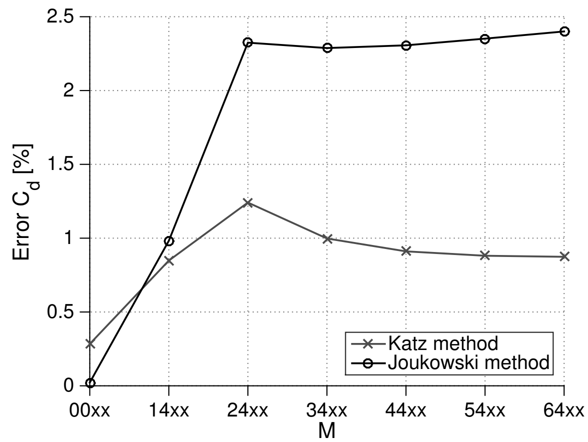

b) Plunge

Figure 3. Errors in pitch and plunge at $k = 0.2$ for different wing profiles of $AR = 4$ and with 28 chordwise panels.

specific chordwise discretisation ($M = 50$).

D. Comments

As mentioned earlier, the Joukowski method is more computationally expensive; this is especially true in 3D. Fig. 4 plots the variation of computation time with chordwise discretisation for an uncambered finite wing in pitch at $k = 0.2$. The cost of the Joukowski approach is approximately three times higher than that of the Katz technique. The simulations were run on a iMac computer (21.5-inch, Late 2013), using Matlab 2014b and C-language functions compiled as mex files.

The results of the previous section clearly show that the Katz method converges much faster for cambered wings. This phenomenon is due to the position of the points where local flow velocities are computed. Those points are shown schematically in Fig. 5. According to the VLM methodology commonly employed, the wing is split into geometric panels and vortex rings are placed on the quarter-chord of each panel. The collocation points lie on the the 3/4 chord points of the geometric panels. The Katz method calculates the local flow velocity on these collocation points (squares in Fig. 5), while the Joukowski method uses the mid-points of the vortex segments (circles). The spanwise segments lie on the geometric panels but the chordwise segments lie below the geomet-

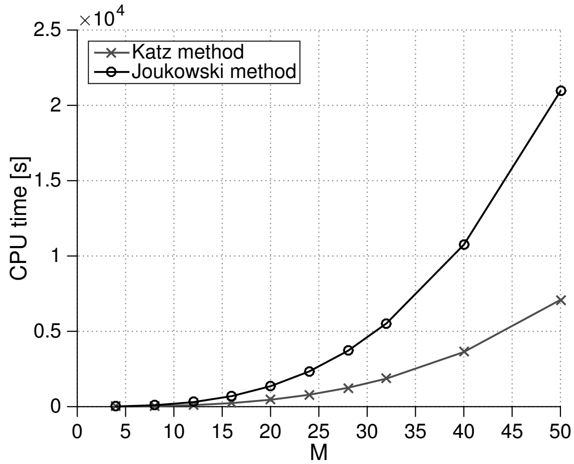

Figure 4. Computation time for a NACA 00xx finite wing in pitch at $k = 0.2$.

ric panels. This means that two of the four points on which the Joukowski method calculates the flow velocity lie very far from the camber line, which explains why this approach converges more slowly than the Katz method as soon as camber is introduced. In the case of a flat plate all the points lie perfectly on the wing, and therefore, the Joukowski approach converges faster.

The placement of the vortex rings on the quarter chord of the geometric panels is a convention that has been commonly employed by the majority of VLM researchers. Moving the vortex rings to the leading edge of the vortex panels would resolve the discretisation error issues that affect the Joukowski method. However such a modification would have to be investigated in detail in order to determine its effects on all aspects of the VLM solution.

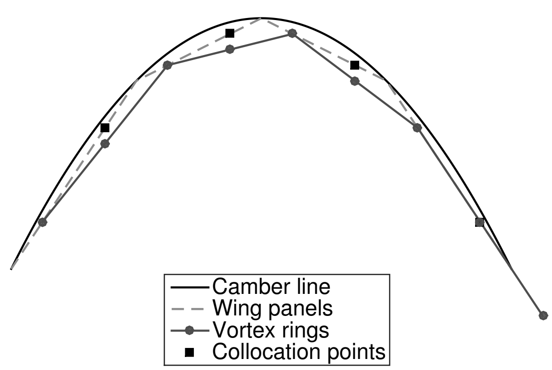

Figure 5. Camber line, wing panels, vortex rings and collocation points .

IV. Conclusions

The Katz and Joukowski approaches for calculating the induced drag of lifting surfaces by the UVLM method were applied to cambered wings. Special attention was drawn to the convergence rate of the drag coefficient with increasing chordwise discretisation for unsteady small oscillations.

For 2D uncambered airfoils, the Joukowski method was found to converge faster than the Katz technique, as already demonstrated by Simpson *et al.* [2]. For cambered airfoils, the Joukowski method converged slightly faster, but only in plunging motion; the Katz method converged faster for pitching motion. The difference in convergence rates decreased with camber, but only in pitch. In general, all convergence rates became slower with increasing camber, due to a poor representation of the cambered surface by linear panels.

In the 3D case, the drag coefficient converged significantly faster with the Joukowski method for the uncambered wing. In contrast, the Katz approach performed much better than the Joukowski technique for all cambered wings. Again, all convergence rates were found to be nearly independent of reduced frequency. The difference in convergence rate was found to increase with camber, making the Katz method even more advantageous at high camber values. It was found that the Joukowski method is less efficient for cambered wings because two of the four points where it calculates the local flow velocity for each panel lie very far from the camber line. This is especially true in 3D, where the number of points far from the camber line is $M * (N + 1)$, while in 2D there are only $2 * M$ such points.

The present work completes the analysis by Simpson *et al.* [2] by investigating the performance of the two methods on cambered wings. Other factors may affect their convergence rates, such as larger amplitudes for the displacements, or geometrical considerations such as taper, sweep, twist etc, but these investigations are beyond the scope of the present note.

References

[1] Katz, J., and Plotkin, A., *Low-Speed Aerodynamics*, Cambridge Univ. Press, Cambridge, England, U.K., 2001, pp 369-447.

[2] Simpson, R. J. S., Palacios, R., and Murua, J., "Induced-Drag Calculations in the Unsteady Vortex Lattice Method," *AIAA Journal*, Vol. 51, No. 7, July 2013, pp. 1775, 1779. doi:10.2514/1.J052136

[3] Garrick, I. E., "Propulsion of a Flapping and Oscillating Airfoil," NACA, Rept. 567, 1937.

[4] Theodorsen, T., "General Theory of Aerodynamic Instability and the Mechanism of Flutter," NACA, Rept. 496, 1935.

[5] Pesmajoglou, S. D., and Graham, J. M. R., "Prediction of Aerodynamic Forces on Horizontal Axis Wind Turbines in Free Yaw and Turbulence," *Journal of Wind Engineering and Industrial Aerodynamics*, Vol. 86, No. 1, 2000, pp. 1-14. doi:10.1016/S0167-6105(99)00125-7

This is the final manuscript accepted by the AIAA.
The published version can be found on AIAA website.

doi:10.2514/1.J055135.